

Regulation of CCl₄-induced liver cirrhosis by hepatically differentiated human dental pulp stem cells

Tomomi Yokoyama¹, Hiromi Yagi Mendoza¹, Tomoko Tanaka¹, Hisataka Ii¹, Riya Takano¹, Ken Yaegaki¹
and Hiroshi Ishikawa¹

¹Nippon Dental University, School of Life Dentistry at Tokyo, Department of Oral Health, 1-9-20, Fujimi,
Chiyoda-ku, Tokyo 102-8159, Japan

Email:

Tomomi Yokoyama, yokoya-t@tky.ndu.ac.jp

Hiromi Yagi, yagi@tky.ndu.ac.jp

Tomoko Tanaka, t-tanaka@tky.ndu.ac.jp

Hisataka Ii, ii-h08@tky.ndu.ac.jp

Riya Takano, rtakano@tky.ndu.ac.jp

Ken Yaegaki, michiyo-y@tky.ndu.ac.jp

Hiroshi Ishikawa, ishi-hiro@tky.ndu.ac.jp

Address correspondence to:

Ken Yaegaki, DDS, PhD, Professor and Head, Department of Oral Health, Nippon Dental University, 1-9-

20 Chiyoda-ku, Tokyo 102-8159, Japan.

Tel: +81-3-3261-8791;

Fax: +81-3-3261-8796

E-mail: michiyo-y@tky.ndu.ac.jp

Abstract

Liver transplantation is the most effective treatment for treating liver cirrhosis. However, a limited number of donors, graft rejection, and other complications can undermine transplant success. It is considered that cell transplantation is an alternative approach of liver transplantation. We previously developed a protocol for hepatic differentiation of cluster of differentiation 117+ stem cells isolated from human exfoliated deciduous tooth pulp (SHEDs) under hydrogen sulfide exposure. These cells showed excellent hepatic function. Here, we investigated whether hepatocyte-like cell transplantation is effective for treating carbon tetrachloride (CCl₄)-induced liver cirrhosis. SHEDs were hepatically differentiated, which was confirmed via immunological analyses and albumin concentration determination in the medium. Rats were intraperitoneally injected with CCl₄ for and the differentiated cells were injected into rat spleen. Histopathological and immunohistochemical analyses were performed. Liver functions were serologically and pathologically determined. Quantitative real-time-polymerase chain reaction was implemented to clarify the treatment procedure of liver cirrhosis. *In vitro*-differentiated hepatocyte-like cells were positive for all examined hepatic markers. SHED-derived hepatocyte transplantation eliminated liver fibrosis and restored liver structure in rats. Liver immunohistochemical analyses showed the presence of human-specific hepatic markers, *i.e.*, a large amount of human hepatic cells were very active in the liver and spleen. Serological tests revealed significant liver function recovery in the transplantation group. Expression of genes promoting fibrosis increased after cirrhosis induction but was suppressed after transplantation. Our

results suggest that xenotransplantation of hepatocyte-like cells of human origin can treat cirrhosis.

Moreover, cell-based therapy of chronic liver conditions may be an effective option.

Keywords: Cell transplantation; Liver cirrhosis;; Tooth pulp stem cells; Hepatic differentiation; Hydrogen sulfide

Acknowledgments

This study was funded by the Nippon Dental University. We also thank Masanori Nasu and Tetsuro Horie, Research Center for Odontology, School of Life Dentistry, Nippon Dental University.

This is a post-peer-review, pre-copyedit version of an article published in *Human Cell*. The final authenticated version is available online at: <http://dx.doi.org/10.1007/s13577-018-00234-0>.

Conflict of Interest

The authors have no competing interest.

Introduction

Liver cirrhosis is the most advanced stage of irreversible chronic liver conditions and can result in fatal liver failure, for which the only available treatment option is organ transplantation [1]. This approach has many challenges, including critical donor shortages, complicated criteria for inclusion or exclusion for transplantation, and severe reactions caused due to the surgery [1,2]. Organ transplantation itself is very critical operation, only limited number of the candidates are accepted [1,2].

Transplantation of undifferentiated stem cells has been well-investigated as an alternative to organ transplantation [3,4]. However, stem cell transplantation (e.g., CD34+ cells) does not treat the liver condition in large number of clinical studies [3,4]. Such cells, however, can potentially form tumors or cause other abnormalities [5,6], although tumor induction has only been reported in the case of embryonic stem cells [7]. Therefore, transplantation of *in vitro*-differentiated stem cells may be safer and more efficient, as reported for cartilaginous differentiation [8]. We previously established a hepatic differentiation protocol for CD117+ human exfoliated deciduous tooth pulp (SHEDs) [9-12]. Tooth pulp can be easily harvested under local anesthesia using routine dental procedures. Exfoliated deciduous teeth are sometimes obtained without anesthesia. Harvesting SHEDs carries a lower risk than bone marrow harvesting [13-15]. SHEDs have characteristics of mesenchymal stem cells (MSCs), consisting of clonogenicity, cell surface antigen

expression, high capacity for cell proliferation, and multi-differentiation potential [16].

SHEDs are a source of cells for cell-based therapies [9-11,16]. Our highly pure hepatocyte-like population differentiated from SHEDs showed excellent liver function, *i.e.*, glycogen storage and production of hepatic marker proteins [9-12]. Previous study demonstrated that the level of hepatic differentiation from SHEDs was higher than that from bone marrow stem cells under hydrogen sulfide (H₂S) exposure, which enhances the function of differentiated hepatocytes [11,12]. We also formulated serum-free medium to avoid complications caused due to biologic products [17]. We found that transplantation of hepatically differentiated SHEDs cured acute liver injury and secondary biliary liver cirrhosis in rats [18]. In this study, we investigated whether transplantation of hepatocyte-like cells derived from SHEDs can treat carbon tetrachloride (CCl₄)-induced cirrhosis in rats.

Materials and methods

Differentiation of CD117+ SHEDs

The study protocol was reviewed and approved by the Research Ethics Committee of Nippon Dental University. Human exfoliated deciduous teeth were procured from children aged 6–12 years who were undergoing routine tooth extraction at collaborating dental clinics and Nippon Dental University Hospital. SHEDs were isolated and cultured, as described previously [12]. CD117+ cells were segregated using

magnetically activated cell sorting immunoselection using a human CD117 MicroBead kit (Miltenyi Biotec GmbH, Bergisch Gladbach, Germany), as previously described [8,14].

Hepatic differentiation

CD117+ SHEDs were expanded 1–2 times and plated in 150 cm² flasks and allowed to reach 70% confluence. To promote hepatic differentiation, our previously reported protocol was employed [11,12]. For 5 days, serum-free DMEM supplemented with 1% insulin-transferrin-selenium-x (ITS-X) (Invitrogen), recombinant human hepatocyte growth factor (HGF) (R&D Systems, Minneapolis, MN, USA), and 100 µg/mL of embryo-trophic factor (ETF) was used as the first differentiation medium. Subsequently, the cells were cultured for 11 days in Iscove's Modified Dulbecco's Medium (Invitrogen) supplemented with ITS-X, HGF, ETF, 10 ng/mL Oncostatin M (R&D Systems), and 10 nmol/L dexamethasone (Wako Pure Chemical Industries) [19-21]. Based on a previous study that reported increased hepatic function following H₂S exposure [11,12], the cells were exposed to 0.1 ng/mL H₂S with 5% CO₂/95% air for 6 days.

Flow cytometry analysis

Flow cytometric analysis was performed as described previously [12] with the following mouse antibodies against human: albumin (Alb) (Sigma–Aldrich), alpha-fetoprotein (αFP) (Santa Cruz Biotechnology, Dallas,

TX, USA), carbamoyl phosphate synthetase (CPS)-1 (Thermo Fisher Scientific, Waltham, MA, USA), hepatocyte nuclear factor (HNF)4 α (Perseus Proteomics, Tokyo, Japan), and insulin-like growth factor (IGF) 1 (Santa Cruz Biotechnology). Alexa Fluor 488-conjugated anti-mouse antibody (Invitrogen) was used as the secondary antibody. The cells were suspended in PBS and analyzed using an EasyCyte flow cytometer (Guava Technologies, Billerica, MA, USA).

Detection of urea via enzyme-linked immunosorbent assay (ELISA)

Given that urea is produced in the liver, the urea concentration in the culture medium was measured with ELISA using a Quanti Chrome Urea Assay kit (BioAssay Systems, Hayward, CA, USA) per the manufacturer's protocol. Culture medium was collected on the last day of differentiation.

Measurement of human Alb concentration in culture medium

After hepatic differentiation, Alb in the differentiation medium after two days of culture was measured using a Human Albumin ELISA kit (Takara Bio, Otsu, Japan) following the manufacturer's instructions.

Fresh differentiation medium was used as a negative control.

Immunocytochemistry and Glycogen storage

Hepatocyte-differentiated cells were fixed and immunostained as described previously [8-10]. The fixed cells were incubated using the following hepatic antibodies: Alb, α FP, CPS-1, IGF, and HNF4 α . The cells were then incubated with Alexa Fluor 568-conjugated anti-mouse and anti-rat secondary antibodies (Life Technologies). The images were obtained with a laser fluorescence microscope (Carl Zeiss AG, Oberkochen, Germany).

After hepatic differentiation, Samples were stained with periodic acid-Schiff (PAS) to confirm glycogen storage, as described previously [10] and observed for glycogen accumulation under a phase-contrast light microscope (Imager M2; Nikon Corporation, Tokyo, Japan).

Animals and treatment

Nine-week-old, male F344/NJcl-rnu/rnu rats ($n = 20$) (Nihon Clea, Tokyo, Japan) were randomized into three groups: transplanted ($n = 6$), control ($n = 6$), and sham group ($n = 8$). In the transplanted and control groups, liver cirrhosis was induced via intraperitoneally injecting 40% CCl₄ in olive oil (Wako Pure Chemical Industries) twice per week for twelfth weeks with a dose of 2.5mL/kg B.W. for the first week and 1.5 ml/kg B.W. for the remaining weeks. These doses were based on those used in previous studies [22,23].

At 5 days after the last dose, the rats were anesthetized and liver biopsy was performed to confirm

cirrhosis. SHEDs derived hepatocytes were resuspended in Hank's Balanced Salt Solution (HBSS; Gibco) at a density of 2.0×10^6 cells/100 μ L. These cells were injected into central regions of the spleens of rats in the transplanted group. Control rats were similarly injected but with 100 μ L HBSS, whereas sham group animals were not injected. The rats were euthanized 4 weeks after transplantation, and the blood, liver, and spleen were collected for analysis.

Collagen staining

Liver tissues were submitted to Masson's trichrome staining, after which the sections were observed using an Imager M2. To confirm morphometric analyses, five different views from each sample were captured and randomly selected to measure fibrous tissue area using the software Image J (NIH, Bethesda, MD, USA).

Immunohistochemistry

Samples were treated with Histo VT One (Nacalai Tesque, Kyoto, Japan), blocked using 0.3% hydrogen peroxide and Blocking One Histo (Nacalai Tesque) to reduce nonspecific antibody interactions. The slides were incubated with monoclonal primary antibodies against human mitochondria (H-Mit) (Abcam, Cambridge, UK), Alb, α FP, IGF, CPS-1, and HNF4 α at 4°C overnight. After washing, specimens were

treated with Mouse on Mouse ImmPRESS Horseradish Peroxidase (Vector Laboratories, Burlingame, CA, USA) for 1 h at room temperature and then reacted with diaminobenzidine horseradish peroxidase substrate (Vector Laboratories). Finally, the slides were visualized under a microscope (FSX 100, Olympus, Tokyo, Japan).

To confirm cell distribution in the liver after transplantation, double fluorescence staining of human Alb and H-Mit was performed. The samples were incubated overnight at 4°C with a goat antibody against human Alb (Abcam) and a mouse antibody against H-Mit; Alexa Fluor 488-conjugated anti-goat (Invitrogen) and Alexa Fluor 568-conjugated anti-mouse were used as secondary antibodies, respectively. Stained slides were analyzed using a laser fluorescence microscope.

Serological tests for liver function

Rat blood serum was separated by centrifugation and utilized for the subsequent serological assays. Alanine Aminotransferase (ALT or SGPT) (BioVision, Mountain View, CA, USA), rat α -fetoprotein/AFP (R&D Systems), rat Total Bilirubin (Cell Biolabs, San Diego, CA, USA), hyaluronic acid (HA) (MyBiosource, San Diego, CA, USA), blood urea nitrogen (BUN) (Cell Biolabs), rat albumin (Abnova, Taipei, Taiwan), and human albumin (Abnova) levels were determined following the manufacturer's protocol.

Real-time quantitative reverse transcription PCR

RNA was extracted from rat liver tissues using the Maxwell[®] RSC Tissue DNA Kit (Promega, WI, USA) and the Maxwell[®] RSC Instrument (Promega) according to the manufacturer's instructions. RNA concentrations were quantified using the NanoVue Plus Spectrophotometer (GE Healthcare, NJ, USA) under RNA detection settings. Extracted RNA was reverse-transcribed to synthesize cDNA using a Veriti 96-Well Thermal Cycler (Applied Biosystems[®], MA, USA) with the RT² First Stand kit (Qiagen, Hilden, Germany), mixed with RT² SYBR[®] Green ROX[™] qPCR Mastermix (Qiagen), and then loaded into the rat fibrosis RT² Profiler PCR Array (Qiagen) as per the manufacturer's protocol. The 84 genes identified through this array are shown in table 1. Cycling conditions for quantitative real-time polymerase chain reaction (qRT-PCR) analyses were 95°C for 10 min, followed by 40 cycles of 95°C for 15 s, and 60°C for 1 min. qRT-PCR was performed using StepOne[™] & StepOnePlus[™] Real-Time PCR Systems (Applied Biosystems[®]). The results were uploaded to and analyzed using RT² Profiler PCR Array Data Analysis version 3.5 (Qiagen) (<http://dataanalysis.sabiosciences.com/pcr/arrayanalysis.php>). Target gene expression levels were normalized against that of *Hprt1* in the sham group. For relative expression analyses, the Δ Ct value was calculated as the difference between the Ct value of *Hprt1* as the housekeeping gene and the target Ct. Fold change ($2^{-\Delta\Delta Ct}$) in gene expression levels was compared between the sham group and control or transplanted group. Each sample underwent three independent experiments.

Statistical analysis

Statistical analyses were performed using the SPSS v.16 for Windows (SPSS, Chicago, IL, USA). Between-group differences were evaluated using the Bonferroni's multiple comparisons test and were considered statistically significant for a *P*-value of <0.05.

Results

Hepatic differentiation

SHEDs had a fibroblast-like spindle shape prior to hepatic differentiation. After differentiation, the cells had the characteristic polygonal morphology of hepatocytes and adhered to the flask surface over a larger area, forming a confluent layer. Cell numbers were decreased compared with the counts before differentiation, changing from 6.5×10^6 to 4.4×10^6 , and the cell viability was 98%.

We analyzed the fraction of cells positive for hepatic markers using flow cytometry and found that 79.6% of cells expressed Alb, 70.3% were positive for α FP, 86.9% for IGF, 82.1% for HNF4 α , and 87.5% for CPS-1, indicating that a highly pure population of hepatic cells was obtained (Fig. 1).

Hepatic function of differentiated cells

Differentiated cells were examined for the expression of hepatic markers Alb, α FP, CPS-1, HNF4 α , and IGF (Fig. 1). Most cells were positive for Alb and α FP. The presence of α FP indicates immaturity of the hepatocytes, but it is also the result of hepatic differentiation. IGF and HNF4 α were also strongly expressed in the cells, and CPS-1 positive granules were detected in the cytoplasm. A large amount of glycogen storage, a typical hepatic function, was also observed (Fig. 2).

The concentration of extracellular urea at the end of hepatic differentiation was 2.6 ± 0.7 mg/dL/ 1.0×10^6 cells. The amount of Alb secreted by the hepatically differentiated cells (1.0×10^5 cells) into the medium was 1.2 ng/day.

Histological recovery of the liver after transplantation

Before cell transplantation, large amounts of collagen were found (Fig. 3a). Thus, the formation of pseudolobules from fibrous tissues was obviously increased. However, the amount of fibrous tissues in the transplanted group rats decreased markedly 4 weeks after the transplantation compared with those in the control group rats; pseudolobules were found to be replaced with regenerative nodules. In contrast, a large amount of fibrous tissue was still observed in control group rats. The number of blood vessels and small bile ducts with irregular shape increased in the control group (Fig. 3b). The fibrosis tissue area was morphologically quantified as a percentage of the entire area. This revealed a significant difference between

the transplanted and control groups. Fibrous area was clearly reduced in the transplanted rats compared with group rats (Fig. 3c).

Immunohistochemical analysis showed several cells in the transplanted group expressing H-Mit and the human-specific liver markers Alb, IGF, α FP, CPS-1, and HNF4 α . In particular, cells near blood vessels were positive for all markers (Fig. 4a-f). A limited number of cells were positive for the markers, because the markers are secreted proteins. Some cells in the bile ducts expressed both H-Mit and human Alb (Fig. 4a,b). Hepatic cells from CD117+ SHEDs were transplanted into the spleen; cells positive for hepatic markers were detected in the spleen of all test rats (Fig. 4g,h), and 50%–70% of spleen tissues were recognized as human hepatic tissues without the bile duct. There were no cells positive for human hepatic markers in the control group (Fig. 4i,j). As shown in Fig. 4k, the tissue was positive to H-Mit antibody whereas negative control was not stained with H-Mit antibody (Fig. 4l). The same tissue was stained by HE (Fig.4m). Hepatic cords composed of human hepatocyte-like cells were observed. The cords were confirmed in most of the liver tissue. These results indicated that the staining was carried out correctly. Double immunofluorescence studies showed that all of the cells reacted with the H-Mit antibody in the transplanted liver injured using CCl₄, whereas human Alb was found only in some of the cells as identified using Alb single staining (Fig. 4n).

Recovery of liver function

ALT concentration was the lowest in the sham group (31.3 ± 3.3 ng/mL) (Fig. 5), and it was significantly lower in the transplanted group (346.7 ± 11.7 ng/mL) than in the control group (1477.1 ± 63.1 ng/mL). α FP concentration was the lowest in the sham group (5.1 ± 0.6 ng/mL), followed by the transplanted group (29.4 ± 3.2 ng/mL); the highest concentration was observed in the control group (92.6 ± 3.9 ng/mL). ALT and α FP concentrations were much lower in the transplanted group than in the control group.

Total bilirubin concentration was distinctively lower in the transplanted group than in the control group. HA concentration was the lowest in the sham group, and it was lower in the transplanted group than in the control group. The opposite trend was observed for BUN level because healthy animals had a higher BUN level. BUN level was higher in the transplanted group than in the control group (Fig. 5).

Rat Alb concentration was low in the transplanted group and the control group. In contrast, human Alb was expressed at approximately 70% of total Alb in the transplanted group. Given that the transplanted hepatocyte-like cells produced a large amount of human Alb in the rat liver, considerable amount of human hepatic tissue was regenerated (Fig. 6).

qRT-PCR of the genes associated with liver fibrosis induction

To normalize qRT-PCR data, one of the housekeeping genes provided in the array, *Hprt1*, was selected for

this study [24]. To determine which signal transduction pathways or factors contributed to establishing CCl₄-induced cirrhosis, the gene expression levels described below were determined. We analyzed gene expression levels between sham and control group (Fig. 7).

Among pro- and anti-fibrotic genes, *Acta2*, *Bcl2*, and *Ccl11* were upregulated in the controls compared to the sham group. *Acta2* was expressed in liver cirrhosis and is known to induce wound healing in cirrhosis [25]. *Bcl-2* (anti-apoptotic factor) activity was enhanced in the control group [26].

Expression of inflammatory cytokine and chemokine genes was also determined. *Il1a* and *Cxcr4* were increased following cirrhosis induction [27]. Expression levels of the *Il1a* family, which are pro-fibrotic factors, were also increased. Expression of signal transduction pathway genes was determined before and after cirrhosis induction. Expression of fibrosis factors, *i.e.*, *Jun*, *Dcn*, *Stat6*, *Nfkb1*, *Tigf1*, *Smad3*, *Myc*, and *Thbs1* was increased after induction whereas only *Inhbe* was decreased. Gene expression of extracellular matrix and cell adhesion molecules was determined. *Lox*, *Mmp8*, *Mmp9*, *Mmp14* and *Serpine1* expressions were upregulated in the control group (non-transplanted group) compared to sham group. This indicates that the above genes are involved in the induction of cirrhosis in rats (Fig. 7).

qRT-PCR of the genes associated with response to treatment using hepatic transplantation

To determine which signal transduction pathways or factors were affected due to the cirrhosis treatment,

expression of the genes described below were determined. The gene expressions of transplanted and control group were compared.

Among the pro- and anti-fibrotic genes, expression levels of *Acta2*, *Bcl2*, *Ccl11*, and *Ccl12* were markedly decreased during treatment; the levels of these genes (except *Ccl12*) were increased during the induction of the condition (Fig. 8).

Gene expression of inflammatory cytokines and chemokines was determined. Expression of *Ifng*, *Il5*, *Il10* and *Il13* were decreased. Among the signal transduction mediators, only the levels of *Jun* and *Tgfb2* were decreased, although these genes were found to be expressed intensively after development of the disease. Among extracellular matrix and cell adhesion molecules, *Mmp1*, *Mmp3*, *Mmp8* and *Mmp13* expressions were decreased whereas the *MMPs* and *Itgb8* and *Serpine1* were increased after cirrhosis induction. Among the growth factors, *Ctgf*, *Edn* and *Pdgfb* were decreased (Fig. 8). Significant differences were confirmed.

When the PCR data was normalized using another housekeeping gene, *b2m*, instead of *Hprt1*, results identical to those with *Hprt1* were obtained.

Discussion

The only treatment option available for liver cirrhosis is liver transplantation [1,2,28]. The surgery, however,

is not always successful [1,2], because lethal postoperative complications may occur [2,29,30]. Moreover, transplantation of a liver from a living donor may lead to the donor's death or severe complications [2,31], although transplantation from a living donor is typically more effective and has a better outcome than donation after circulatory death [32]. Stem cell transplantation (e.g., CD34+ cells) [3] does not offer a cure, but it may delay the progress of the condition during the waiting period involved in organ transplantation [33,34].

We previously reported a protocol for hepatic differentiation of SHEDs and demonstrated that exposure to H₂S increased hepatic function [11,12]. Moreover, grafting hepatically differentiated cells alleviated acute liver injury and secondary biliary liver cirrhosis [18].

In the present study, we investigated whether the condition could be treated by transplanting hepatically differentiated CD117+ SHEDs into a CCl₄-induced liver cirrhosis rat model. CD117+ cells are presumed to represent a hepatic progenitor cell population that can promote liver tissue repair [35] and that has multilineage differentiation potential [9,10,12,36,37]. Thus, CD117+ tooth pulp cells are an important cell source for cell-based therapy.

The differentiated cells were positive for all the hepatic markers including Alb, α FP, IGF, HNF4 α , and CPS-1 and for glycogen storage, indicating that they functioned as hepatocytes [9–12,18]. We also confirmed the presence of human Alb in the culture medium after hepatocytic differentiation. A previous

study reported only the relative ratio of human Alb after hepatic differentiation from human induced pluripotent stem cells (iPSCs) [38]. Without absolute Alb values, hepatic differentiation cannot be determined, because stem cells also produce Alb definitively [10,12]. Forbes *et al.* reported that hepatic differentiation from iPSCs was a critical hurdle [39]. Our results demonstrate that hepatocyte-like cells produce a certain amount of human Alb, indicating that a large amount of human hepatic tissue was regenerated as seen morphologically.

Hepatocytes derived from iPSCs or bone marrow-derived stem cells (BMCs) have been intravenously transplanted into mice with CCl₄-induced cirrhosis [40–42]. However, transplantation into the vein or liver can result in engraftment of cells in other tissues [39]. It is expected that such ectopic cells would be removed by natural killer cells [43], which was suggested by the presence of lymphocytes in Fig. 3. To circumvent this possibility, we performed intrasplenic transplantation, because ES cells or SHEDs were previously transplanted successfully into the spleen in animal models of CCl₄-induced cirrhosis [44]. In previous studies, hepatocytes differentiated from ES cells, BMCs, or human umbilical cord MSCs were intrasplenically transplanted into rats with CCl₄-induced cirrhosis using a protocol similar to ours [44–46].

Engrafted hepatocytes derived from SHEDs produced human-specific proteins and liver markers. ALT was upregulated in the control group, whereas the opposite was observed in the transplanted group. Liver inflammation was reduced after transplantation. Since serum albumin concentration was recovered, the engraftment of human hepatocyte-like cells in the rat's liver may contribute to the changes seen in liver

function tests of serum. Specially human albumin may subsidize to recovering liver function, rather than rat hepatocytes as shown in Fig. 6. α FP is known to be elevated in liver carcinoma or cirrhosis but is also a hepatic marker during differentiation [47]. Large quantities of α FP is not secreted from mature hepatocytes. The transplanted cells in our study may be well differentiated, hence α FP was decreased. Bilirubin concentration decreased after transplantation. The peripheral bile duct may be regenerated as shown in Fig. 4a and b, then the liver function was recovered. In fact, we observed human cells in the bile duct epithelium of rats in the transplanted group. We described the fate of hepatocyte-like cells immunologically and serologically. Serological analyses clearly indicated that the cells engrafted into rats completely functioned as liver cells; this was because the differentiated cells were well-regenerated human hepatocyte-like cells. Another reason could have been that the bile duct was partially reproduced by human cells, although bile duct regeneration has not yet been reported. Therefore, bilirubin was reduced to the standard level after transplantation.

The production of fibrous tissues induced by CCl_4 was dramatically reduced to a level comparable with that in the sham group, which promoted liver function as well as bile duct regeneration. Rats in the transplanted group were immunopositive for all human-specific hepatic markers. Cells expressing these markers surrounded the blood vessels, indicating that human cells from the spleen entered the liver through the portal vein. This process might be the key issue in regenerating the liver continuously. Since the cells transplanted showed a very positive response to human Alb, we are able to confirm that they

are human hepatocyte-like cells. Moreover, bile duct walls stained positive for H-Mit and human Alb may suggest the presence of progenitor cells producing both hepatocyte-like cells and bile duct cells.

Gene analyses provided interesting suggestions. The basis for *Ccl11* expression is not yet clear, with conflicting functional data reported. *Ccl11* (Eotaxin) is detected in liver diseases, especially drug induced-hepatic conditions, and induces fibrosis [48]. One function promotes the condition, but another inhibits it. *Jun*, an anti-apoptotic factor, is also a pro-fibrosis factor. *Dcn*, *Stat6*, *Nfkb1*, *Tigif1*, *Smad 3*, *Myc*, and *Tgfbr2* are also fibrosis factors or inducers of cirrhosis [49-54]. The members of *Il1a* family are pro-fibrotic factors, and they also promote liver regeneration [28,55]. It is not yet known how these factors function in the animal model we used. They might broadly promote the condition or inhibit the healing process.

On the other hand, gene analyses clearly indicated that levels of pro-fibrotic genes, *i.e.*, *Acta2*, *Bcl2*, and *Ccl11* were increased after cirrhosis induction, but all pro-fibrotic genes decreased after transplantation. As indicated by the results of PCR array, the anti-fibrosis genes were up-regulated by transplanted group compared to control group. Activation of these genes were considered to improve liver fibrosis. Identical changes were seen in levels of *Il6*, *Jun*, *Tgfbr2*, and *MMPs*. These data indicate that transplantation may be able to influence these genes and treat cirrhosis.

The present study showed that transplantation of hepatocyte-like cells derived from SHEDs

resulted in regeneration of cirrhotic rat livers, indicating clear recovery from the condition. Given that rat liver histology is not completely representative of that of large animals, including humans, the rat cirrhosis model may not resemble human cirrhosis. Studies in larger animal models are required to address this problem and perform more detailed investigations.

Compliance with ethical standards

Funding

This study was partially funded by Research Project No. 3 from Nippon Dental University, Tokyo, Japan.

Ethical approval

All procedures performed in studies involving human participants were in accordance with the ethical standards of the institutional and/or national research committee of Nippon Dental University School of Life Dentistry at Tokyo as well as the 1964 Helsinki declaration and its later amendments or comparable ethical standards. Informed consent was obtained from all individual participants and their parents/LAR included in the study. All procedures performed in studies involving animals were in accordance with the ethical standards of the institution or practice at which the studies were conducted.

References:

1. Murray KF, Carithers RL Jr, AASLD. AASLD practice guideline: evaluation of the patient for liver transplantation. *Hepatology*. 2005; 41: 1407-32.
2. Lo CM. Complications and long-term outcome of living liver donors: a survey of 1,508 cases in five Asian centers. *Transplantation*. 2003; 75: S12-5.
3. Feldmann G. Liver transplantation of hepatic stem cells: potential use for treating liver diseases. *Cell Biol Toxicol*. 2001; 17: 77-85.
4. Nakamura T, Koga H, Iwamoto H et al. Ex vivo expansion of circulating CD34(+) cells enhances the regenerative effect on rat liver cirrhosis. *Mol Ther Methods Clin Dev*. 2016; 3: 16025.
5. Crowder SW, Horton LW, Lee SH et al. Passage-dependent cancerous transplantation of human mesenchymal stem cells under carcinogenic hypoxia. *FASEB J*. 2013; 27: 2788-98.
6. Curtis RE, Rowings PA, Deeg HJ et al. Solid cancers after bone marrow transplantation. *N Engl J Med*. 1997; 336: 897-904.
7. Zhu W, Xu W, Jiang R et al. Mesenchymal stem cells derived from bone marrow favor tumor cell growth in vivo. *Exp Mol Pathol*. 2006; 80: 267-74.

8. Akay I, Oxmann D, Helfenstein A et al. Tumor risk by tissue engineering: cartilaginous differentiation of mesenchymal stem cells reduces tumor growth. *Osteoarthritis Cartilage*. 2010; 18: 389-96.
9. Ishkitiev N, Yaegaki K, Calenic B et al. Deciduous and permanent dental pulp mesenchymal cells acquire hepatic morphologic and functional features in vitro. *J Endod*. 2010; 36: 469-74.
10. Ishkitiev N, Yaegaki K, Imai T et al. High-purity hepatic lineage differentiated from dental pulp stem cells in serum-free medium. *J Endod*. 2012; 38: 475-80.
11. Ishkitiev N, Calenic B, Aoyama I, Ii H, Yaegaki K, Imai T. Hydrogen sulfide increases hepatic differentiation tooth pulp stem cells. *J Breath Res*. 2012; 6: 017103.
12. Okada M, Ishkitiev N, Yaegaki K et al. Hydrogen sulfide increases hepatic differentiation of human tooth pulp stem cells compared with human bone marrow stem cells. *Int Endod J*. 2014; 47: 1142-50.
13. Bain BJ. Bone marrow aspiration. *J Clin Pathol*. 2001; 54: 657-63.
14. Bain BJ. Bone marrow biopsy morbidity: review of 2003. *J Clin Pathol*. 2005; 58: 406-8.
15. Chahla J, Mannava S, Cinque ME, Geeslin AG, Codina D, LaPrade RF. Bone marrow aspirate concentrate harvesting and processing technique. *Arthrosc Tech*. 2017; 6: e441-5.
16. Miura M, Gronthos S, Zhao M et al. SHED: stem cells from human exfoliated deciduous teeth. *Proc Natl Acad Sci USA*. 2003; 100: 5807-12.

17. Hirata TM, Ishkitiev N, Yaegaki K et al. Expression of multiple stem cell markers in dental pulp cells cultured in serum-free media. *J Endod.* 2010; 36: 1139-44.
18. Ishkitiev N, Yaegaki K, Imai T et al. Novel management of acute or secondary biliary liver conditions using hepatically differentiated human dental pulp cells. *Tissue Eng Part A.* 2014; 21: 586-93.
19. Michalopoulos GK, Bowen WC, Mulè K, Luo J. HGF-, EGF-, and dexamethasone-induced gene expression patterns during formation of tissue in hepatic organoid cultures. *Gene Expr.* 2003; 11: 55-75.
20. Suzuki A, Iwama A, Miyashita H, Nakauchi H, Taniguchi H. Role for growth factors and extracellular matrix in controlling differentiation of prospectively isolated hepatic stem cells. *Development.* 2003; 130: 2513-24.
21. Kamiya A, Gonzalez FJ. TNF-alpha regulates mouse fetal hepatic maturation induced by oncostatin M and extracellular matrices. *Hepatology.* 2004; 40: 527-36.
22. Iredale JP, Benyon RC, Pickering J et al. Mechanisms of spontaneous resolution of rat liver fibrosis. Hepatic stellate cell apoptosis and reduced hepatic expression of metalloproteinase inhibitors. *J Clin Invest.* 1998; 102: 538-49.
23. Jiang Y, Wang C, Li YY et al. Mistletoe alkaloid fractions alleviates carbon tetrachloride-induced liver fibrosis through inhibition of hepatic stellate cell activation via TGF- β /Smad interference. *J Ethnopharmacol.* 2014; 158 Pt A: 230-38.

24. Svingen T, Letting H, Hadrup N, Hass U, Vinggaard AM. Selection of reference genes for quantitative RT-PCR (RT-qPCR) analysis of rat tissues under physiological and toxicological conditions. *PeerJ*. 2015; 3:e855.
25. Rockey DC, Weymouth N, Shi Z. Smooth muscle α actin (Acta2) and myofibroblast function during hepatic wound healing. *PLoS One*. 2013; 8: e77166.
26. Frommel TO, Yong S, Zarling EJ. Immunohistochemical evaluation of Bcl-2 gene family expression in liver of hepatitis C and cirrhotic patients: a novel mechanism to explain the high incidence of hepatocarcinoma in cirrhotics. *Am J Gastroenterol*. 1999; 94: 178-82.
27. Pham BN, Bemau J, Durand F et al. Eotaxin expression and eosinophil infiltrate in the liver of patients with drug-induced liver disease. *J Hepatol*. 2001; 34: 537-47.
28. Tan Q, Hu J, Yu X et al. The role of IL-1 family members and Kupffer cells in liver regeneration. *Biomed Res Int*. 2016; 2016: 6495793.
29. Cholongitas E, Marelli L, Shusang V et al. A systematic review of the performance of the model for end-stage liver disease (MELD) in the setting of liver transplantation. *Liver Transpl*. 2006; 12: 1049-61.
30. Elkholy S, Mogawer S, Hosny A et al. Predictors of mortality in living donor liver transplantation. *Transplant Proc*. 2017; 49: 1376-82.
31. Berglund D, Kirchner V, Pruett T et al. Complications after living donor hepatectomy: analysis of 176

cases at a single center. *J Am Coll Surg.* 2018; 227: 24-36.

32. Wakade VA, Mathur SK. Donor safety in live-related liver transplantation. *Indian J Surg.* 2012; 74: 118-26.

33. Kling CE, Perkins JD, Reyes JD, Montenovo MI. Living donation versus donation after circulatory death liver transplantation for low MELD recipients. *Liver Transpl.* 2018; 10: doi: 10.1002/lt.25073.

34. Terai S, Ishikawa T, Omori K et al. Improved liver function in patients with liver cirrhosis after autologous bone marrow cell infusion therapy. *Stem Cells.* 2006; 24: 2292-98.

35. Nakamura T, Torimura T, Iwamoto H et al. CD34(+) cell therapy is safe and effective in slowing the decline of hepatic reserve function in patients with decompensated liver cirrhosis. *J Gastroenterol Hepatol.* 2014; 29: 1830-8.

36. Baumann U, Crosby HA, Ramani P, Kelly DA, Strain AJ. Expression of the stem cell factor receptor c-kit in normal and diseased pediatric liver: identification of a human hepatic progenitor cell? *Hepatology.* 1999; 30: 112-7.

37. Ishkitiev N, Yaegaki K, Kozhuharova A et al. Pancreatic differentiation of human dental pulp CD117⁺ stem cells. *Regen Med.* 2013; 8: 597-612.

38. Okada M, Imai T, Yaegaki K, Ishkitiev N, Tanaka T. Regeneration of insulin-producing pancreatic cells using a volatile bioactive compound and human teeth. *J Breath Res.* 2014; 8: 046004.

39. Takebe T, Sekine K, Enomura M et al. Vascularized and functional human liver from an iPSC-derived organ bud transplant. *Nature*. 2013; 499: 481-4.
40. Forbes SJ, Gupta S, Dhawan A. Cell therapy for liver disease: From liver transplantation to cell factory. *J Hepatol*. 2015; 62: S157-69.
41. Sakaida I, Terai S, Yamamoto N et al. Transplantation of bone marrow cells reduces CCl₄-induced liver fibrosis in mice. *Hepatology*. 2004; 40: 1304-11.
42. Asgari S, Moslem M, Bagheri-Lankarani K, Pournasr B, Miryounesi M, Baharvand H. Differentiation and transplantation of human induced pluripotent stem cell-derived hepatocyte-like cells. *Stem Cell Rev*. 2013; 9: 493-504.
43. Raafat N, Abdel Aal SM, Abdo FK, El Ghonaimy NM. Mesenchymal stem cells: In vivo therapeutic application ameliorates carbon tetrachloride induced liver fibrosis in rats. *Int J Biochem Cell Biol*. 2015; 68: 109-18.
44. Mandal A, Viswanathan C. Natural killer cells: In health and disease. *Hematol Oncol Stem Cell Ther*. 2015; 8: 47-55.
45. Moriya K, Yoshikawa M, Saito K et al. Embryonic stem cells develop into hepatocytes after intrasplenic transplantation in CCl₄-treated mice. *World J Gastroenterol*. 2007; 13: 866-73.
46. Okumoto K, Saito T, Haga H et al. Characteristics of rat bone marrow cells differentiated into a liver

- cell lineage and dynamics of transplanted cells in the injured liver. *J Gastroenterol*. 2006; 41: 62-9.
47. Xue G, Han X, Ma X et al. Effect of microenvironment on differentiation of human umbilical cord mesenchymal stem cells into hepatocytes in vitro and in vivo. *Biomed Res Int*. 2016; 2016: 8916534.
48. Adinolfi A, Adinolfi M, Lessof MH. Alpha-feto-protein during development and in disease. *J Med Genet*. 1975; 12: 138-51.
49. Ma R, Chen J, Li Z, Tang J, Wang Y, Cai X. Decorin accelerates the liver regeneration after partial hepatectomy in fibrotic mice. *Chin Med J (Engl)*. 2014; 127: 2679-85.
50. Kong X, Horiguchi N, Mori M, Gao B. Cytokines and STATs in liver fibrosis. *Front Physiol*. 2012; 3: 69.
51. Luedde T, Schwabe RF. NF- κ B in the liver--linking injury, fibrosis and hepatocellular carcinoma. *Nat Rev Gastroenterol Hepatol*. 2011; 8:108-18.
52. Xu F, Liu C, Zhou D, Zhang L. TGF- β /SMAD Pathway and its regulation in hepatic fibrosis. *J Histochem Cytochem*. 2016; 64: 157-67.
53. Zheng K, Cubero FJ, Nevzorova YA. c-MYC-making liver sick: role of c-MYC in hepatic cell function, homeostasis and disease. *Genes (Basel)*. 2017; 8. pii: E123.
54. Li Y, Turpin CP, Wang S. Role of thrombospondin 1 in liver diseases. *Hepatol Res*. 2017; 47: 186-93.

55. Zhou WC, Zhang QB, Qiao L. Pathogenesis of liver cirrhosis. *World J Gastroenterol.* 2014; 20: 7312-24.

Figure Legends:

Fig. 1

Histograms of a Alb, b α FP, c IGF, d HNF4 α and e CPS-1, detected by using Alexa Fluor 568 as secondary antibody. Red peak shows differentiated hepatocyte-like cells, green color peak shows undifferentiated stem cells

Fig. 2

Immunofluorescence staining of hepatically differentiated CD117+ SHEDs. Nuclei are observed in blue, and hepatic markers detected using specific antibodies are shown in red. **a:** Alb and **b:** α FP were detected in most cells. **c:** IGF and **d:** HNF4 α were strongly labeled. **e:** CPS-1 was visible as punctae. All markers were detected in all analyzed samples. Scale bar = 50 μ m. **f:** Glycogen in the cells was detected using PAS staining (purple). Scale bar = 100 μ m. Alb, human albumin; α FP, alpha-fetoprotein; CPS, carbamoyl phosphate synthetase; HNF, hepatocyte nuclear factor; IGF, insulin-like growth factor; PAS, periodic acid-Schiff; SHEDs, stem cells from human exfoliated deciduous tooth pulp

Fig. 3

a: Pathology of the liver immediately before transplantation and 86 days after CCl₄ treatment. Collagen fibers appear blue after Masson's trichrome staining. Large amounts of collagen were observed in biopsies obtained from CCl₄-treated rats immediately before the transplantation. **b:** Histopathological analysis of liver tissue four weeks after the transplantation of hepatocytes derived from SHEDs. A large amount of remnant fibrous tissue was observed in the control group compared with the transplanted group. Pseudolobules surrounded by thin fibrous tissue were replaced with the regenerated tissue. Scale bar = 100 μm. CCl₄, carbon tetrachloride; SHEDs, stem cells from human exfoliated deciduous tooth pulp. **c:** Quantitative analyses of fibrous areas were performed after Masson trichrome staining. There were significant differences between each group. Five views from each animal were analyzed. Data are presented as mean ± SD. **p* < 0.05

Fig. 4

a-f : Expression of H-Mit, Alb, αFP, IGF, HNF4α, and CPS-1 (brown) in hepatocyte-like cells transplanted into the livers of rats with CCl₄-induced cirrhosis. All human liver markers used, including Alb, were highly expressed near blood vessels. H-Mit and Alb were detected in the bile duct

wall. Hepatocyte-like cells were injected into the spleens of transplanted rats expressing. H-Mit (g) and HNF4 α (h). Immunostaining of the spleens in transplanted rats revealed that approximately 70% of the tissue expressed human hepatic markers. H-Mit (i) and HNF4 α (j) expressions in the spleen of a control rat. No human hepatic marker was detected in the control rat. Expression of H-Mit, (k), negative control (l) and m. HE (m) in the liver of transplanted group. Scale bar = 50 μ m. Alb, human albumin; α FP, alpha-fetoprotein; CCl₄, carbon tetrachloride; CPS, carbamoyl phosphate synthetase; H-Mit, primary antibodies to human mitochondria; HNF, hepatocyte nuclear factor; IGF, insulin-like growth factor. n: Double immunofluorescent staining for H-Mit and Alb. H-Mit was stained green, Alb was stained red

Fig. 5

Changes in liver function in CCl₄-induced cirrhosis after hepatocyte transplantation. ALT, α FP, total bilirubin, and HA concentrations decreased in the transplanted group. Sham group ($n = 8$); Control ($n = 6$); Transplanted ($n = 6$). Data are presented as means \pm SD. * $p < 0.001$. α FP, alpha-fetoprotein; ALT, alanine transaminase; BUN, blood urea nitrogen; CCl₄, carbon tetrachloride; HA, hyaluronic acid

Fig. 6

Alb concentrations in rat serum. Human (2.6 ± 0.2 U/L) and rat (1.2 ± 0.1 U/L) albumin were detected in the serum of the transplanted group rats. Exceptional reduction in rat albumin was observed in the control group. Human-specific albumin was not detected in either control group. Data are presented as mean \pm SD. * $p < 0.001$

Fig. 7

Comparing fibrosis genes expression levels between the livers of sham rats and those of control rats. Pro-fibrotic and signal transduction genes were upregulated. The analyses were performed using RT² Profiler PCR Array Data Analysis version 3.5 (Qiagen). The data are expressed as mean \pm SD. * $p < 0.05$

Fig. 8

Comparing fibrosis genes expression levels between the livers of transplanted group and those of control group. Pro-fibrotic, inflammatory cytokines and extracellular matrix genes clearly decreased. The analyses were performed using RT² Profiler PCR Array Data Analysis version 3.5. The data are expressed as mean \pm SD. * $p < 0.05$

Fig. 1

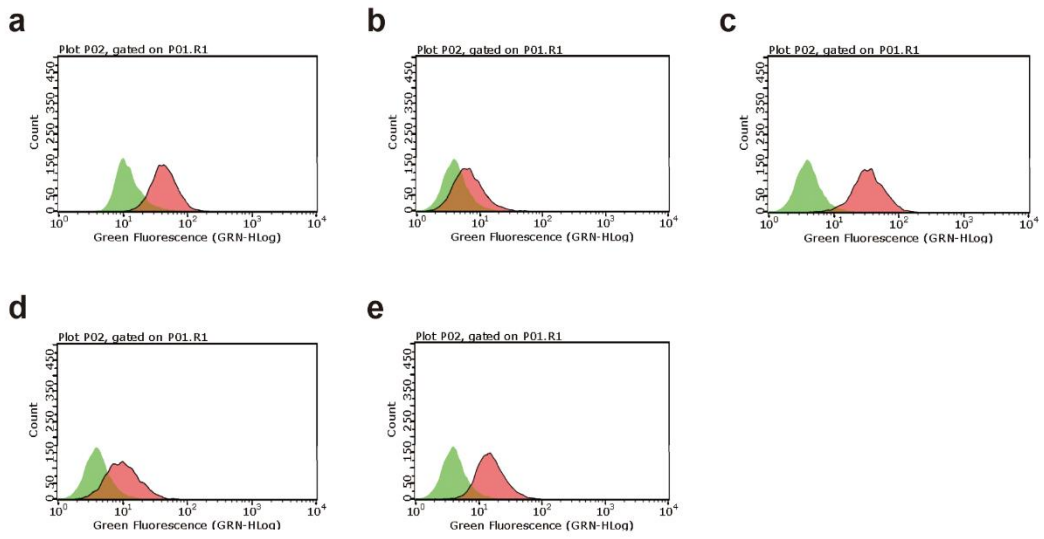


Fig. 2

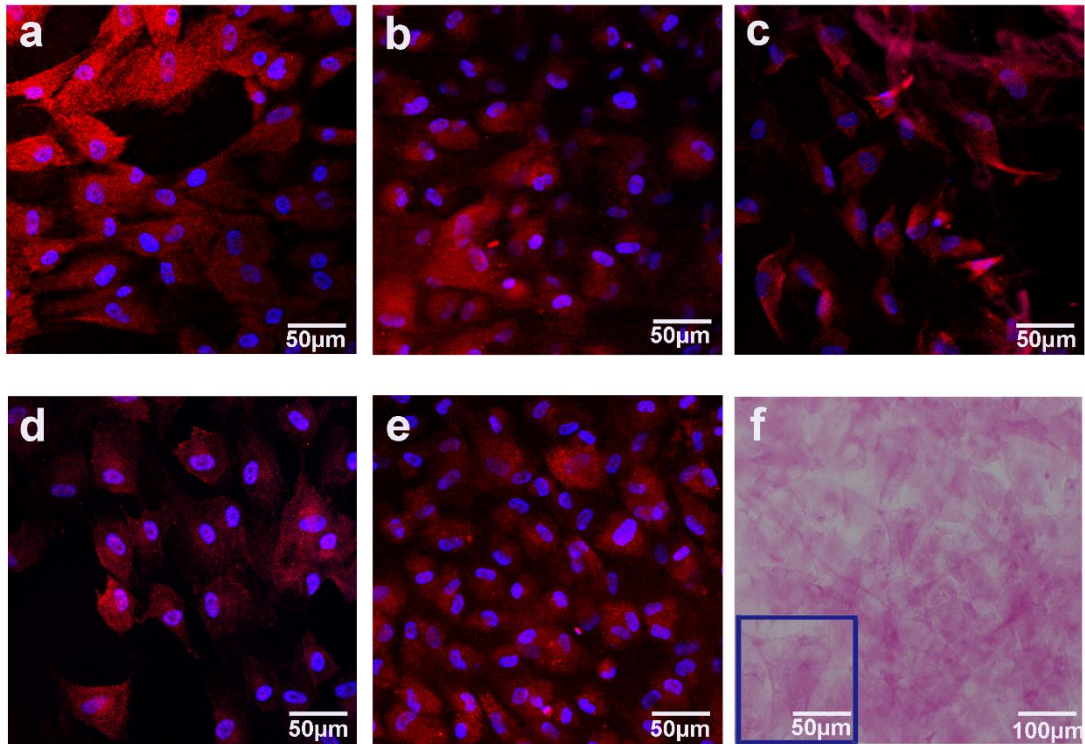
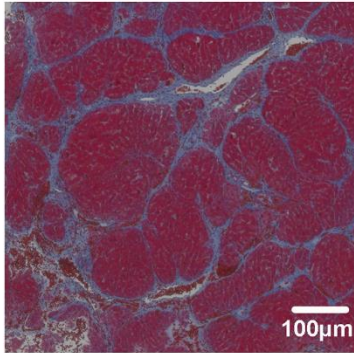
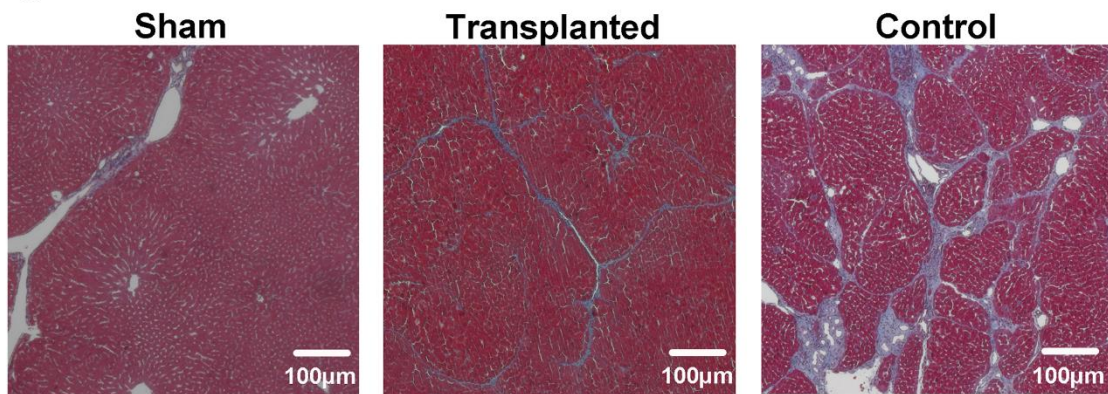


Fig. 3

a



b



c

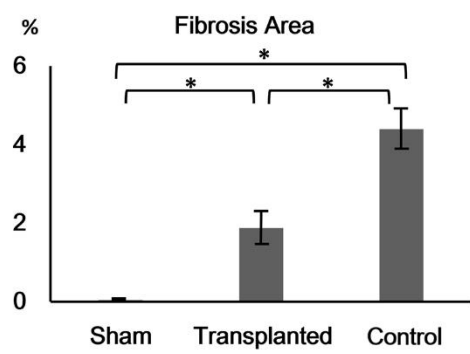
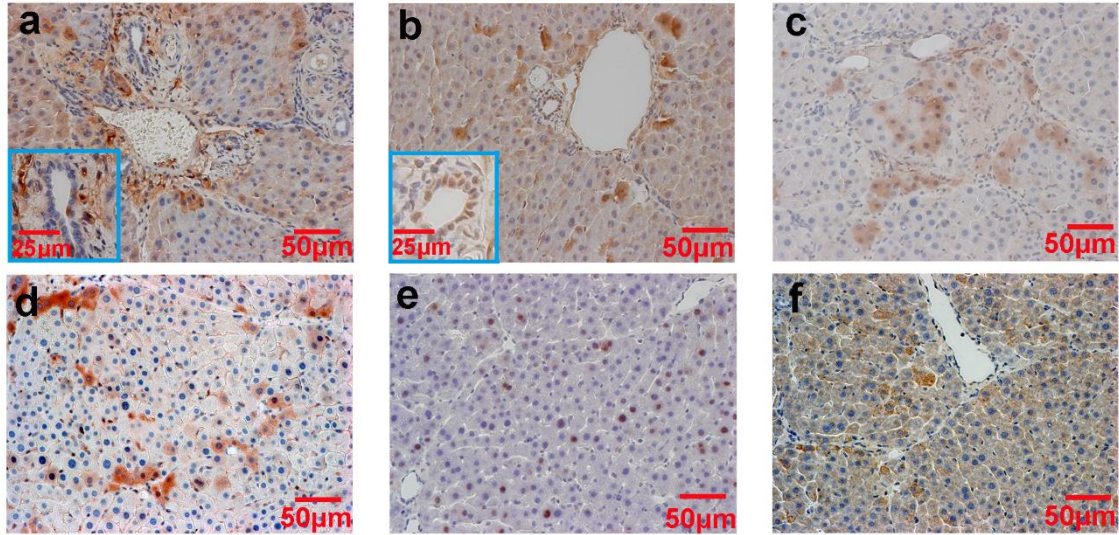
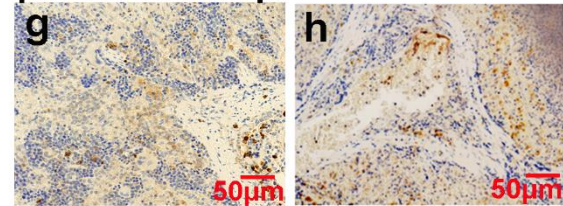


Fig. 4

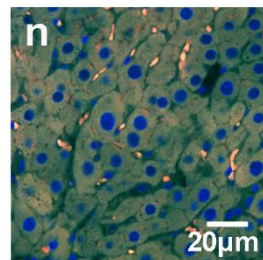
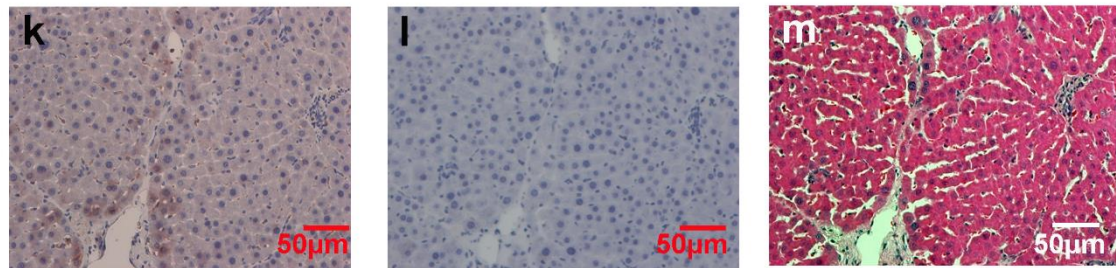
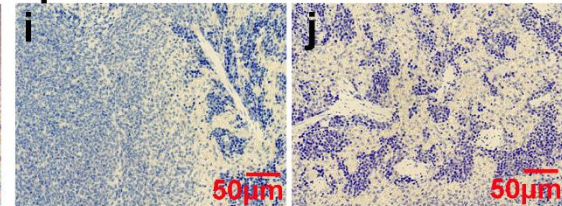
Liver in Transplanted



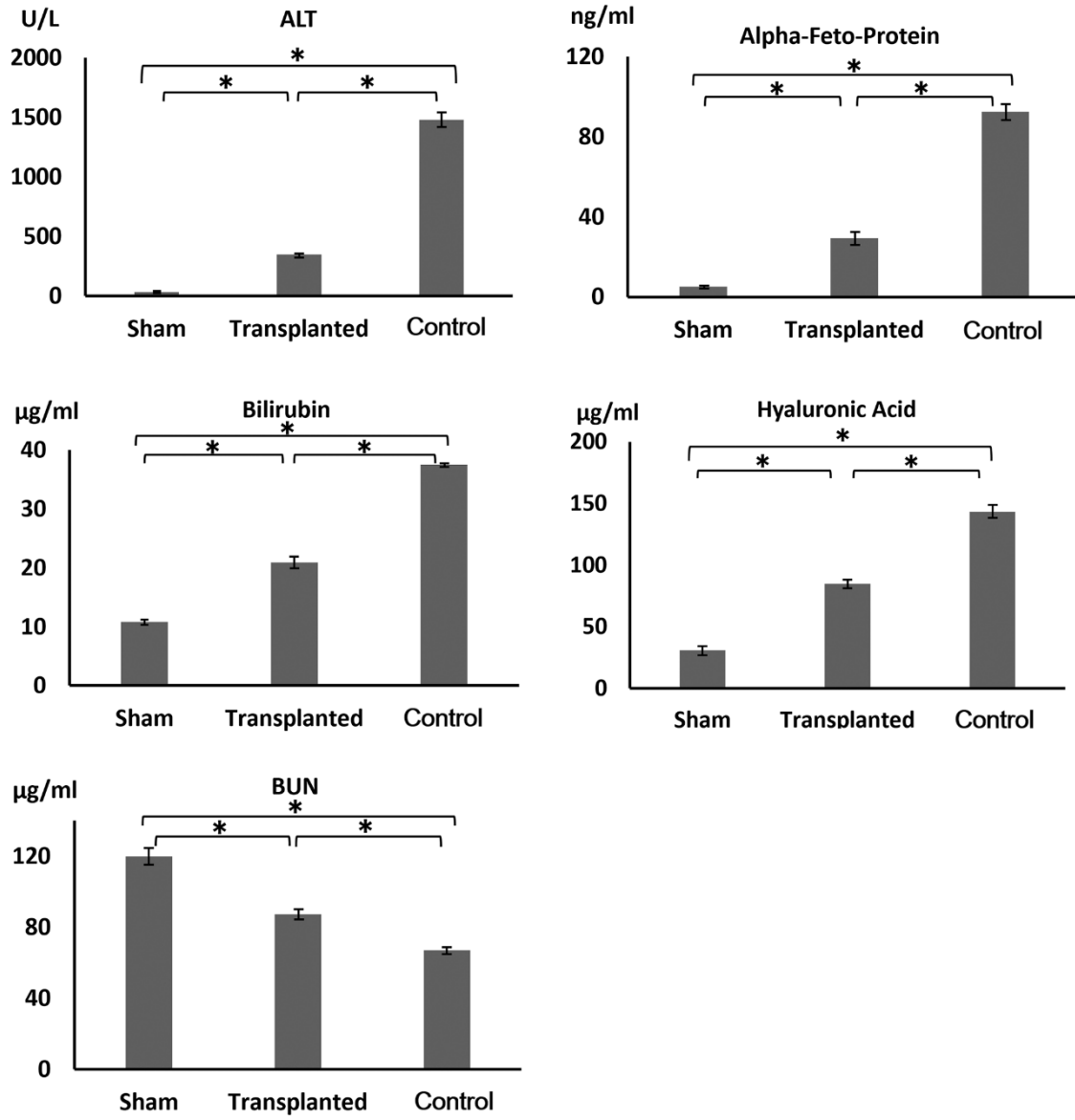
Spleen in Transplanted



Spleen in Control



Fog. 5



Fog. 6

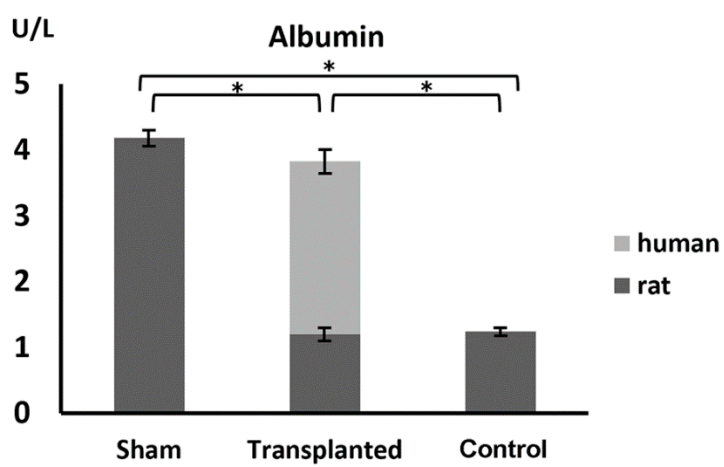


Fig. 7

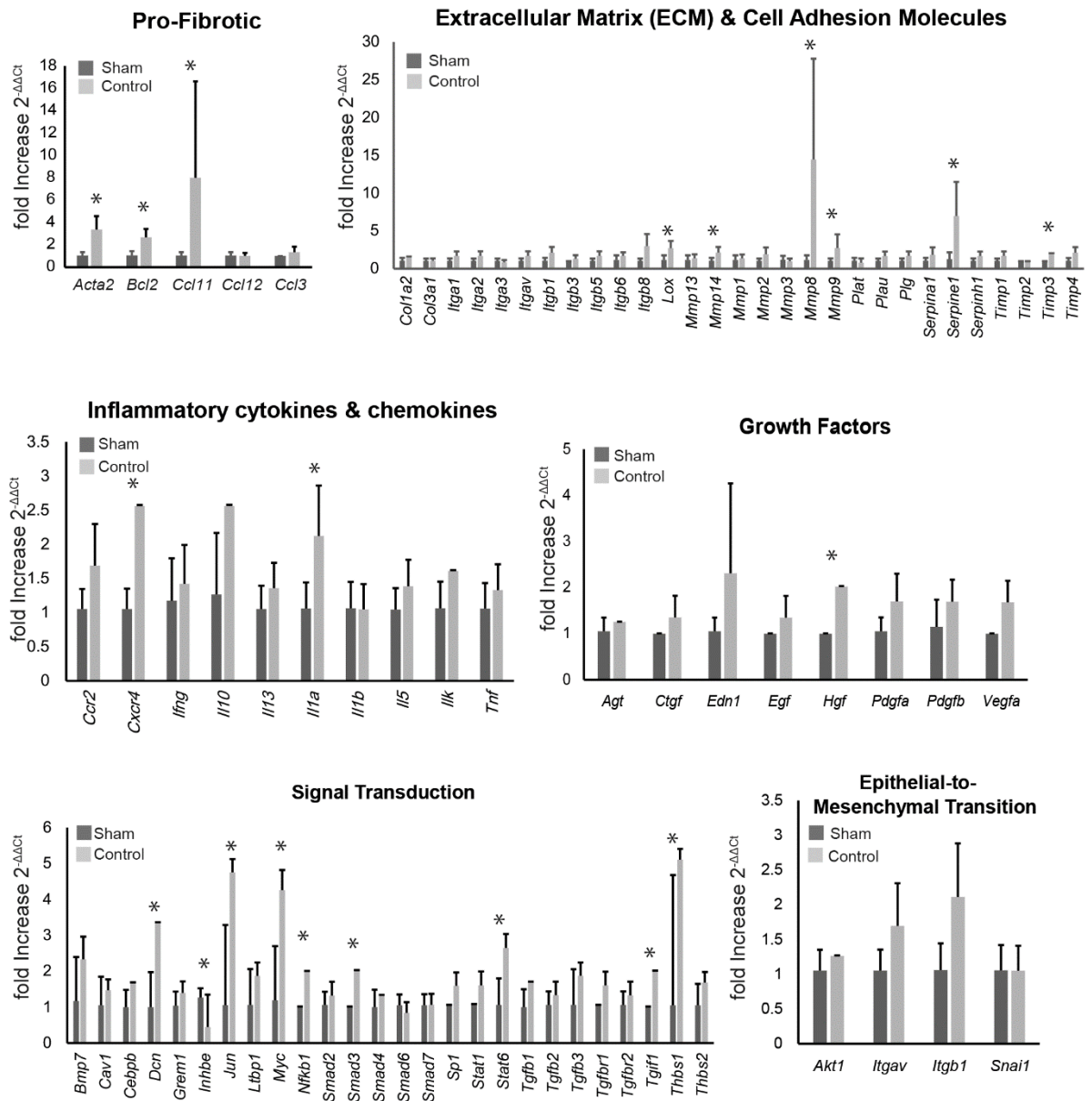


Fig. 8

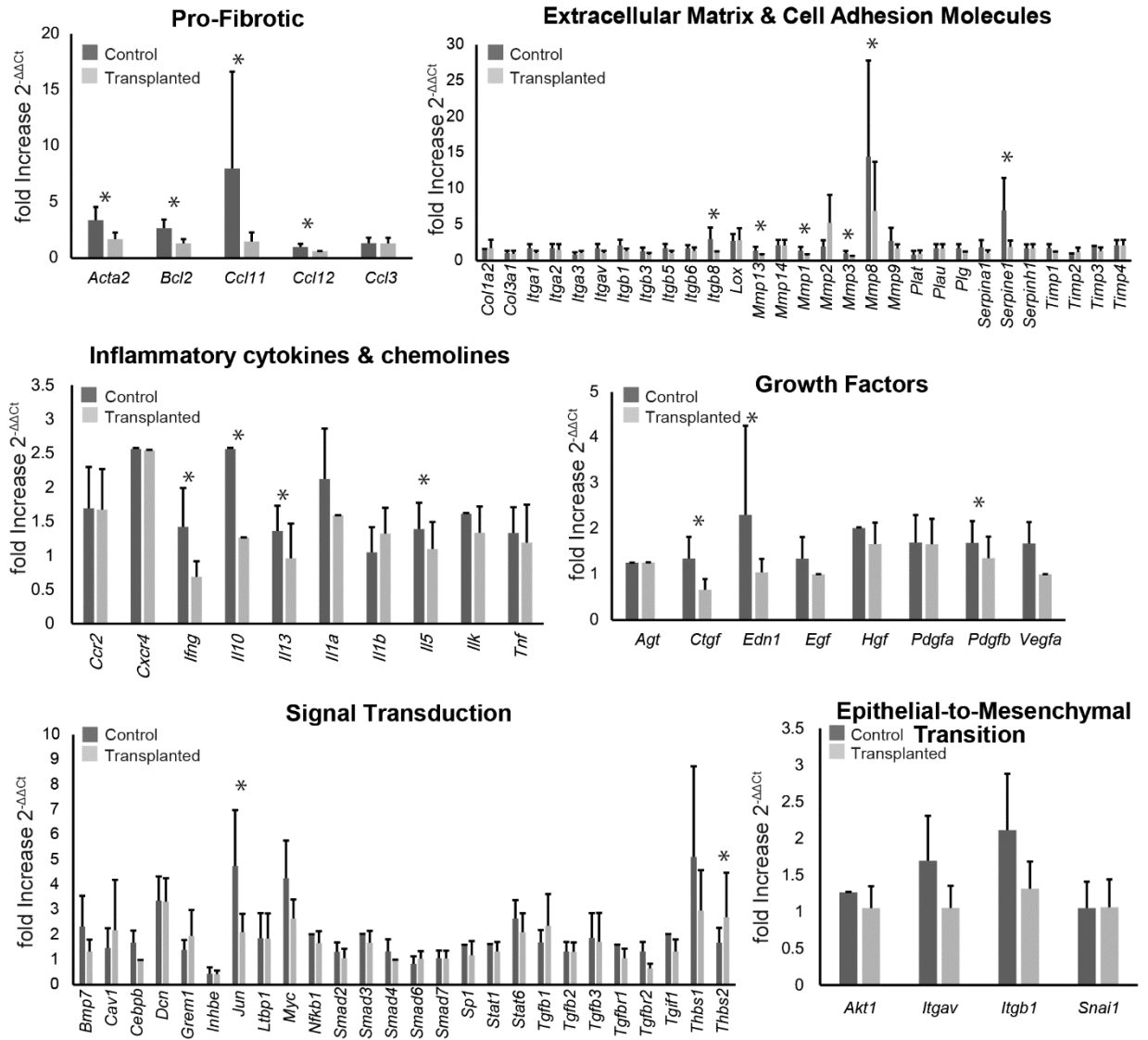


Table. 1 Genes included in RT² profiler PCR Array Rat Fibrosis

PCR Templates	
Symbol	Full Name
Acta2	Actin, Alpha 2, Smooth Muscle, Aorta
Actb	Actin Beta
Agt	Angiotensinogen
Akt1	AKT serine/Threonine Kinase 1
B2m	Beta-2-Microglobulin
Bcl2	B-cell Lymphoma 2 Apoptosis Regulator
Bmp7	Bone Morphogenetic Protein 7
Cav1	Caveolin 1
Ccl11	Cysteine-cysteine Motif Chemokine Ligand 11
Ccl12	Cysteine-cysteine Motif Chemokine Ligand 12
Ccl3	Cysteine-cysteine Motif Chemokine Ligand 3

Ccr2	Cysteine-cysteine Motif Chemokine Receptor 2
Cebpb	Cytosine-cytosine-adenosine-adenosine-thymidine Enhancer Binding Protein Beta
Col1a2	Collagen Type I Alpha 2 Chain
Col3a1	Collagen Type III Alpha 1 Chain
Ctgf	Connective Tissue Growth Factor
Cxcr4	Cysteine-x-cysteine Motif Chemokine Receptor 4
Dcn	Decorin
Edn1	Endothelin 1
Egf	Epidermal Growth Factor
Eng	Endoglin
Faslg	Fas Ligand
Grem1	Gremlin 1
Hgf	Hepatocyte Growth Factor
Hprt1	Hypoxanthine Phosphoribosyltransferase 1
Ifng	Interferon Gamma
Il10	Interleukin 10
Il13	Interleukin 13

Il13ra2	Interleukin 13 Receptor Subunit Alpha 2
Il1a	Interleukin 1 Alpha
Il1b	Interleukin 1 Beta
Il4	Interleukin 4
Il5	Interleukin 5
Ilk	Integrin Linked Kinase
Inhbe	Inhibin Subunit Beta E
Itga1	Integrin Subunit Alpha 1
Itga2	Integrin Subunit Alpha 2
Itga3	Integrin Subunit Alpha 3
Itgav	Integrin Subunit Alpha V
Itgb1	Integrin Subunit Beta 1
Itgb3	Integrin Subunit Beta 3
Itgb5	Integrin Subunit Beta 5
Itgb6	Integrin Subunit Beta 6
Itgb8	Integrin Subunit Beta 8
Jun	Jun Proto-Oncogene
Ldha	Lactate Dehydrogenase A

Lox	Lysyl Oxidase
Ltbp1	Latent Transforming Growth Factor Beta Binding Protein 1
Mmp1	Matrix Metallopeptidase 1
Mmp13	Matrix Metallopeptidase 13
Mmp14	Matrix Metallopeptidase 14
Mmp2	Matrix Metallopeptidase 2
Mmp3	Matrix Metallopeptidase 3
Mmp8	Matrix Metallopeptidase 8
Mmp9	Matrix Metallopeptidase 9
Myc	Myc Proto-Oncogene, Basic Helix-Loop-Helix Transcription Factor
Nfkb1	Nuclear Factor Kappa B Subunit 1
Pdgfa	Platelet Derived Growth Factor Subunit A
Pdgfb	Platelet Derived Growth Factor Subunit B
Plat	Plasminogen Activator, Tissue Type
Plau	Plasminogen Activator, Urokinase
Plg	Plasminogen
Rplp1	Ribosomal Protein Lateral Stalk Subunit P1

Serpina1	Serpin Family A Member 1
Serpine1	Serpin Family E Member 1
Serpinh1	Serpin Family H Member 1
Smad2	Mothers Against Decapentaplegic Homolog2
Smad3	Mothers Against Decapentaplegic Homolog3
Smad4	Mothers Against Decapentaplegic Homolog4
Smad6	Mothers Against Decapentaplegic Homolog6
Smad7	Mothers Against Decapentaplegic Homolog7
Snai 1	Snail Family Transcriptional Repressor 1
Sp1	Specificity Protein 1 Transcription Factor
Stat1	Signal Transducer And Activator Of Transcription 1
Stat6	Signal Transducer And Activator Of Transcription 6
Tgfb1	Transforming Growth Factor Beta 1
Tgfb2	Transforming Growth Factor Beta 2
Tgfb3	Transforming Growth Factor Beta 3
Tgfb1	Transforming Growth Factor Beta Receptor 1
Tgfb2	Transforming Growth Factor Beta Receptor 2
Tgif1	Transforming Growth Factor Beta Induced Factor Homeobox 1

Thbs1	Thrombospondin 1
Thbs2	Thrombospondin 2
Timp1	Tissue Inhibitor of Metalloproteinase Metallopeptidase Inhibitor 1
Timp2	Tissue Inhibitor of Metalloproteinase Metallopeptidase Inhibitor 2
Timp3	Tissue Inhibitor of Metalloproteinase Metallopeptidase Inhibitor 3
Timp4	Tissue Inhibitor of Metalloproteinase Metallopeptidase Inhibitor 4
Tnf	Tumor Necrosis Factor
Vegfa	Vascular Endothelial Growth Factor A